Cement and Concrete Research 185 (2024) 107645

Contents lists available at ScienceDirect

Cement and Concrete Research

journal homepage: www.elsevier.com/locate/cemconres

Enhancing structural efficiency with digital concrete – Principles, opportunities and case studies

Lukas Gebhard [a,1], Jaime Mata-Falcón [b,*,1], Rebecca Ammann [a], Nadine Preßmair [c], Benjamin Kromoser [c], Costantino Menna [d], Abtin Baghdadi [e], Harald Kloft [e], Michael Gabriel [f], Martin Walch [g], Walter Kaufmann [a]

[a] Institute of Structural Engineering, ETH, Zurich, Switzerland
[b] Department of Continuum Mechanics and Theory of Structures, Universitat Politècnica de València, Spain
[c] Institute of Green Civil Engineering, University of Natural Resources and Life Sciences, Austria
[d] Department of Structures for Engineering and Architecture, University of Naples Federico II, Italy
[e] Institute of Structural Design, Technische Universität Braunschweig, Germany
[f] Concrete 3D GmbH, Austria
[g] Tragwerk ZT GmbH, Austria

ARTICLE INFO

Keywords:
Digital concrete
Concrete structures
Structural efficiency
Environmental sustainability
Optimisation

ABSTRACT

This paper explores the opportunities of digital fabrication with concrete (DFC) to improve structural efficiency and achieve sustainable construction. Efficient structural solutions that drastically reduce material consumption can be achieved by ensuring direct load flow and placing material where needed. More than 50 % of material savings can be achieved by using flanges or hollow sections, providing continuity in beams or slabs, reducing the span of structures or using structural systems such as arches, trusses or deep beams. These concepts are not fully exploited as they often require expensive and complex formwork. DFC tackles the latter point, as it promises to produce complex geometries, minimising extra effort, cost, or waste. The paper discusses the optimisation potential of DFC for several structural elements and presents existing applications that demonstrate this potential. Five case studies of different technological approaches are discussed in detail, highlighting advantages and disadvantages to be addressed for widespread adoption.

1. Introduction

Faced with the current climate crisis and the significant contribution of the building sector - accounting for 37 % of energy-related CO_2 emissions [1] - the construction industry must implement more environmentally friendly practices. These new practices are particularly necessary in the context of a growing global population, increasing living standards, and ageing infrastructure that will keep pushing construction activity. The environmental impact of any structure depends on four key factors: (i) the impact of the construction material per mass, (ii) how much of this material is required to create a usable space, (iii) the amount of usable space needed for its intended purpose, and (iv) the overall service life ([2] adapted from [3], see Fig. 1.1).

Presuming that current living standards shall be maintained, sustainability in construction is thus achievable through (i) using materials with minimal environmental impact, (ii) maximising the efficiency of the structures (build more with less), and (iii) ensuring a long service life and circular practices. While discussions for a more sustainable future in construction focus on construction materials, the potential lever of building more with less has received comparatively little attention. However, the sustainability of construction can be drastically enhanced by implementing structural systems that minimise material consumption overall or facilitate the use of sustainable, lower-strength materials without sacrificing structural performance. Such structural systems are referred to as material-efficient, resource-efficient, or just structurally efficient.

In addition to the levers of material and structure, manufacturing techniques must be considered to reach sustainable construction [4]. Naturally, these levers are interrelated: Advancements in concrete or reinforcement material technology directly lead to possible or necessary

* Corresponding author at: Universitat Politècnica de València, Camino de Vera, s/n 46022, Spain.
E-mail address: jmata@mes.upv.es (J. Mata-Falcón).
[1] Both authors contributed equally to this manuscript.

https://doi.org/10.1016/j.cemconres.2024.107645
Received 29 March 2024; Received in revised form 14 August 2024; Accepted 15 August 2024

adaptations of the structural concrete element dimensions as well as respective manufacturing processes.

While advanced knowledge and tools for designing efficient structures are readily available, manufacturing these structures is challenging, as they often require expensive and complex formwork. Digital fabrication with concrete (DFC) might overcome this lacuna regarding concrete structures. DFC is an overall term for new technologies to produce concrete structures with innovative and minimal, or even without any formwork, promising to produce complex geometries without (much) extra effort, cost, or waste [5]. However, to date, most of these technologies have not lived up to that promise, as (i) the used materials typically have a higher environmental impact than those used in conventional processes [3] and (ii) the use cases are mainly limited to structures with little optimisation potential, such as walls [6]. However, the field of DFC is still young, and the technologies are under development. Therefore, exploring all the possibilities of the new technologies is crucial to best inform new developments.

This paper explores the opportunities and challenges of DFC in achieving sustainable construction by building with higher structural efficiency and lower material use. While a wide range of materials are involved in construction (insulation, flooring, cladding, etc.), the scope is limited to the material efficiency of concrete structures. After an overview of historical developments of efficient constructions, the paper introduces general design principles and examines current DFC approaches for fabricating structural elements efficiently. The potential and limitations of DFC are highlighted through five case studies.

2. Historical perspective on efficient concrete structures

The concrete-like materials predominantly used by the Romans (stone, *opus caementitium*) could only resist significant loads in compression, leading to the extensive use of arches and vaults [7], which are highly efficient for compression structures under permanent loads. However, their mass (and hence, material use) had to be increased to ensure a state of compression for other loading scenarios. On the other hand, beams were restricted to relatively short spans when built in stone, as in the Greek temples. Arch and vault structures were used for many centuries until the advent of modern high-strength building materials (concrete and steel), particularly during the 19th century. The combination of concrete (strong in compression but comparatively weak and subjected to large scatter in tension) with reinforcing steel (strong and ductile in compression and tension) opened the way for more slender designs: the thickness of arches and vaults could be reduced since the thrust line (compressive resultant force) no longer needed to remain inside the cross-section, and beams became available for large spans. The introduction of prestressing further increased the achievable spans of reinforced concrete structures. Prestressing allows compensating for permanent loads and prevents cracks in most load scenarios, thereby significantly reducing deformations.

Between the end of the 19th to the first half of the 20th century, the new knowledge about the material and structural behaviour, together with a very high cost (partly driven by scarcity during war times) of building materials with respect to manual labour – which made it possible to economically produce formwork for complex geometries – enabled a golden age of efficient concrete structures, spearheaded by luminaries such as Robert Maillart (1872–1940), Pier Luigi Nervi (1891–1979), Eduardo Torroja (1899–1961), and Felix Candela (1910–1997) [8]. With the increase in labour costs in developed countries, such structurally efficient designs became uneconomical and were abandoned for the sake of efficient – cheap and fast – construction (see Fig. 2.1). Instead, geometrically simple, labour-cost-efficient, and reusable formwork systems, including straightforward solutions for building systems and services, became standard. Unfortunately, this focus on minimising manual labour led to a significant and ongoing increase in material usage. However, there is growing pressure to increase structural efficiency as one of the levers towards more ecological structures.

3. Principles for structural efficiency

The basis for achieving structural efficiency lies in straightforward principles: (i) ensuring a direct load transfer and (ii) placing material with pertinent material properties where needed. While implementing such material-efficient structures is specific to the given boundary conditions, these principles are generally valid and will be illustrated in the following using a series of straightforward examples. Despite that this is essentially textbook knowledge, highlighting the tremendous potential of structural efficiency to minimise material consumption is worthwhile, as it is often underestimated.

A distributed load q is assumed, whereby uniform and partial loading configurations are considered. The self-weight and second-order effects are neglected, and only normal forces and bending moments are considered. In all cases, the dimensions of the cross-sections are determined to reach the same magnitude of the maximum normal stress for linear elastic behaviour and are considered constant over the length of the element. Note that for compact cross-sections made of ductile material, higher efficiencies could be achieved by considering plastic bending resistances (enabling the activation of the full material strength over the entire cross-section); this is, however, not further considered here. Three levels of adaptation impacting the material consumption in the structure are studied: (i) changes in the support conditions, (ii) changes in the cross-section, and (iii) changes in the structural system.

Fig. 3.1 illustrates the effect of changing the support conditions from (left) a simply supported beam to (centre) a clamped beam and (right) two simply supported beams with half the span each. Clamping both ends of the beam (b) results in hogging moments at the supports and reduces the moment at mid-span, enabling savings of 24 % compared to the simply supported beam. This support condition can be reached by bending stiff connections or ensuring continuous, multi-span beams. Reducing the span of the simply supported beam to a half (c) ensures a more direct load transfer, resulting in only a quarter of the bending moment for uniform load and enabling material savings of 60 %.

While changes in the support conditions cause changes in the internal actions, varying the geometry of the cross-section causes changes in the resistance. Assuming linear elastic material behaviour, the bending resistance of a cross-section is defined by its elastic section modulus W and the magnitude of maximum normal stress. The bending moment is most efficiently resisted by placing the material as far from the neutral axis as possible, which is illustrated in Fig. 3.2: by changing the height-to-width ratio of the cross-section from one (square section) to two (upright rectangle), 21 % of the material can be saved (Fig. 3.2a). Fig. 3.2b highlights the effect of different cross-section shapes, indicating the change in elastic modulus W and area A compared to a reference square cross-section. Note that the larger dimension of the rectangular and flanged cross-sections has been chosen to correspond to

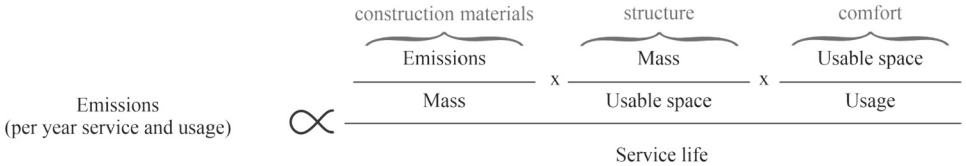

Fig. 1.1. Environmental impact of construction works per service year and usage ([2] adapted from [3]).

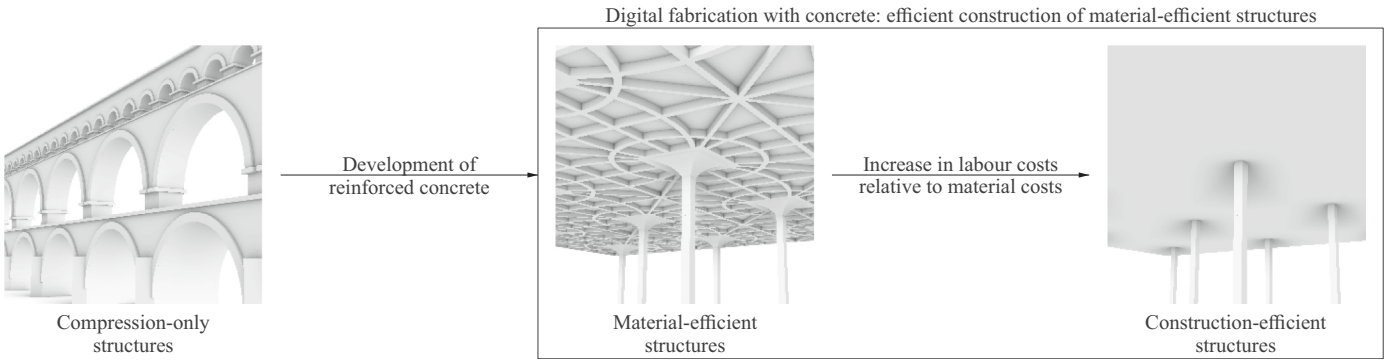

Fig. 2.1. Schematic development of concrete structures over time.

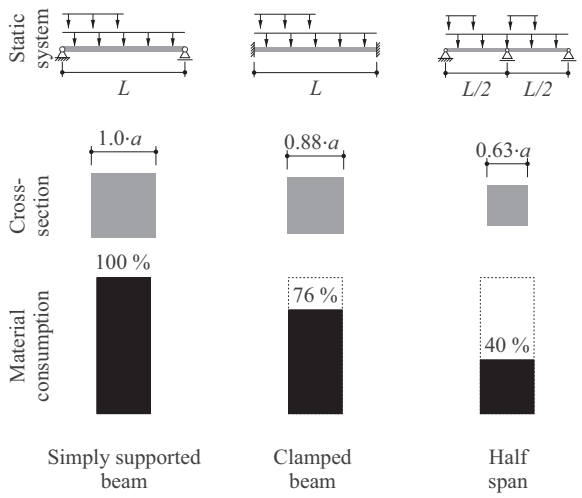

Fig. 3.1. Structural efficiency through changes in the support conditions: cross-section and material consumption for square beams with different support conditions and identical load-bearing capacity.

the side length of the reference square cross-section, whereas the outer diameter of the circular and annular cross-sections has been determined such that the full section has the same area as the reference square cross-section. In the flanged and annular cross-sections, the material is allocated near the top and bottom, increasing the elastic section modulus W for a given area. Consequently, reducing the total area, hence material use, corresponds to a much less pronounced reduction of the resistance with respect to the reference cross-section (e.g. strength reduction by merely 15 % for a flanged cross-section and 37 % for an annular cross-section with 50 % of the area). In contrast, in rectangular cross-sections with reduced depth, the material is lumped near the neutral axis, and hence, reducing the total area disproportionately impairs the resistance (e.g. reduction by 75 % with 50 % of the area). For rectangular cross-sections with reduced width, the ratio between the resistance and the total area is constant (i.e. 50 % resistance at 50 % total area).

While for the considered example, the self-weight of the structure was neglected, it is often dominant in real structures. Optimising the cross-section is thus even more beneficial since the applied load and the internal actions diminish along with the material savings. If only self-weight is considered, the bending moment is proportional to the cross-sectional area A. Hence, the ratio W/A is decisive. This ratio is plotted in Fig. 3.2c. For a pure stringer cross-section (infinitesimally small flange thickness), this ratio would be three times higher than for a square cross-section with the same height, highlighting the efficiency of flanged cross-sections. For real applications, a web is needed in addition to the flanges to transmit shear forces, leading to I-cross-sections as widely used in steel construction. When dealing with slabs rather than beams, ribbed slabs and hollow-core slabs are well-known typologies showing high material efficiency following that logic.

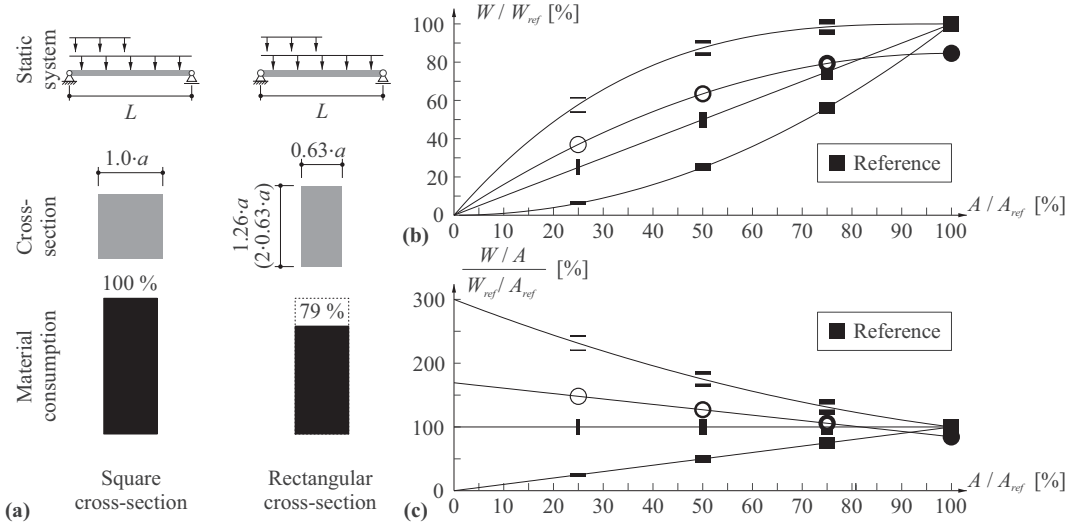

Fig. 3.2. Structural efficiency through changes in cross-section: (a) square and rectangular simply supported beams with identical load-bearing capacity; (b) and (c) elastic modulus W to cross-section area A, and ratio of elastic modulus of the cross-section W to cross-section area A with respect to a reference square cross-section considering four cross-section typologies (rectangular with constant width and reduced depth, rectangular with constant depth and reduced width, annular, flanged).

A further increase in structural efficiency can be achieved by providing more structural depth while reducing material used by the web (either with a narrow cross-section or a different structural system), as illustrated in Fig. 3.3. This figure compares possible solutions ensuring the same load-bearing capacity as the reference beam with a square cross-section (Figs. 3.1 and 3.2). With a simply supported, very narrow rectangular beam with a depth of $L/4$ (which corresponds to around six times the depth of the square cross-section of the reference beam), a drastic material reduction by around 83 % can be achieved. These savings could even be enhanced by featuring a varying depth to adapt to the acting bending moments. However, this solution would hardly be constructible and susceptible to stability issues for the given height-to-width ratio of around 200 to 1. However, the same load-bearing capacity can be maintained while further reducing material consumption by feasible material-efficient structural systems such as a tied arch (material reduction by around 91 % under symmetric loading) or a truss (material reduction by around 87 % under equivalent point loads), provided that lateral stability of the compression chords is ensured. For the tied arch under symmetric loading and the truss under equivalent point loads, all structural elements are loaded in pure normal forces, allowing full material strength to be used over the entire cross-sections (without requiring plastic redistribution). However, when considering half-span loading for the tied arch and a uniform load for the truss, respectively, bending moments occur in the arch and the top flange of the truss in addition to the normal forces. Even when considering these bending moments, however, drastic material reductions by around 67 % and 73 % can still be achieved for the tied arch and the truss, respectively.

While trusses and arches have been known to be efficient structural systems for decades (see Section 2), the research interest in numerical methods to optimise structures under various boundary conditions has grown in the past few years. In particular, topology optimisation allows the efficient arrangement of material within a given design space related to defined performance criteria [9]. Fig. 3.4 shows examples of concrete designs achieved with topology optimisation using different software tools [10]. The designs obtained with these sophisticated methods resemble traditional structural systems such as the truss and tied arch presented beforehand, highlighting the general applicability of the underlying principles of efficient material placement and direct force flow.

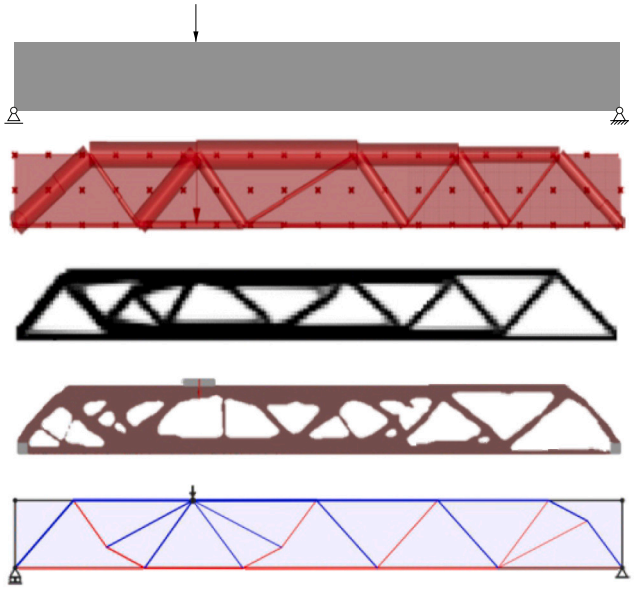

Fig. 3.4. Example of structural optimisation through topology optimisation (adapted from [10]).

More details on topology optimisation will be given in the respective case studies in Section 5.

More complex geometries and correspondingly laborious fabrication processes (as for the tied arch and truss shown in Fig. 3.3), need for connections with a high performance (as for the clamped beam shown in Fig. 3.1), or the introduction of additional supports potentially affecting the use (as for the beam with half span shown in Fig. 3.1). Furthermore, stability problems and second-order effects, which were not accounted for in the considered examples, generally become more significant with increasing structural efficiency, diminishing some potential material savings. Therefore, the shown examples should be viewed as indicating a general trend rather than being taken at face value.

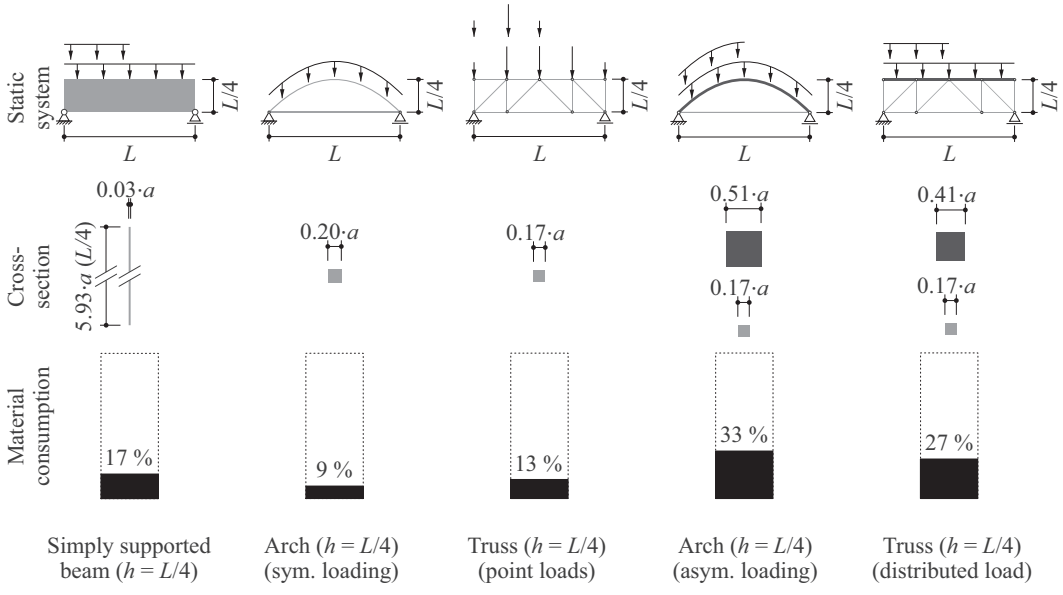

Fig. 3.3. Structural efficiency through changes in structural systems: cross-section and material consumption for different structural systems with identical load-bearing capacity and depth at midspan. Left to right: simply supported beam, tied arch with symmetrical loading, truss with point loads, tied arch with symmetrical and asymmetrical loading, truss with distributed load. (Material consumption referred to the simply supported beam with a square cross-section shown in Figs. 3.1 and 3.2).

4. Opportunities of DFC towards structural efficiency

4.1. Overview of DFC technologies

In conventional concrete construction, the formwork is placed first. Afterwards, the reinforcement is installed, and the concrete is cast. Therefore, the form is defined by the formwork, and any complexity of the final shape must be reflected in the formwork and partly in the reinforcement. For complex geometries, this leads to excessive manual labour and costs. DFC tries to rethink conventional concrete construction by automating one or multiple steps [5]. Some technologies aim to produce elements without any formwork, while others apply non-conventional formwork either temporarily or stay-in-place [11].

The most widely applied DFC technology is 3D concrete printing (3DCP) or contour crafting [12], where a fine mortar is extruded from a nozzle, fabricating an element layer by layer. Instead of extruding, the concrete can also be automatically sprayed either in layers (Shotcrete 3D printing (SC3DP)) or into formwork [13,14]. Non-conventional formwork can be produced with extruded polymer 3D printing [15,16], binder jet printing or particle bed printing [17]. Instead of providing formwork for the entire structure, Smart Dynamic Casting (SDC) describes a slipforming process for vertical elements, i.e. columns, using short and adjustable formwork elements [11,18]. Another type of formwork is knitted textiles allowing straightforward production of surfaces with double curvatures and integration of ribs and channels. This concept was developed into KnitCrete, where a tensioned knitted textile is sprayed with a hardening agent to obtain a stable formwork for concrete [19]. The automation of the reinforcement production is the basis of the Mesh Mould technology [20,21], where a complex and closely spaced reinforcement cage simultaneously acting as formwork is fabricated.

These technologies have been used to fabricate various structural elements. The structural elements considered in the following are columns, walls, beams (incl. single-span bridges), and slabs. It should be noted that other structural elements or civil structures, such as wind turbine towers [22] and foundations [23], might offer large savings potentials. However, as there are limited examples of such structures, they are not be considered further. Additionally, joining - especially for prefabrication - is crucial to go from structural elements to full structures. Here, DFC offers various possibilities for rethinking the geometry and location of connections [24–27]. However, a detailed discussion of these aspects is out of the scope of this paper.

4.2. Columns

Columns are mainly subjected to compressive normal forces. Therefore, in contrast to elements primarily loaded in bending, the distance of the material from the neutral axis is less relevant for the resistance. However, bending occurs due to second-order effects and monolithic connection to slabs or frames, which limits the slenderness of columns. In this case, hollow cross-sections are theoretically more efficient just as in girders loaded in bending. However, in contrast to steel columns or reinforced concrete bridge piers, which are typically built with hollow cross-sections, concrete columns in buildings are commonly produced with full cross-sections to minimise dimensions. Hence, there is limited structural optimisation potential in columns (despite that DFC has been applied to produce mullions, i.e. essentially vertical beams, with varying cross-sections and to explore new aesthetics [28,29]). At the intersection of columns and slabs, however, DFC can be leveraged: high hogging moments in the slab combined with the locally introduced column reactions can lead to punching shear failure, and mushroom slabs can be used to substantially enhance structural efficiency. While they complicate conventional formwork, mushroom slabs have been efficiently produced with 3DCP [30] and SC3DP [14]. A similar column-slab transition was produced with the Eggshell technology [31].

4.3. Walls

While columns have mainly a structural function, walls - especially in residential housing, except for core walls ensuring horizontal stability - must primarily fulfil other requirements, such as partitioning or thermal and acoustic insulation. Therefore, they have limited potential for increased structural efficiency, as other requirements are often governing. Nevertheless, the 3D concrete printing of unreinforced residential walls - resembling unreinforced masonry - has been one of the main applications in the industry [32,33]. The potential for structurally demanding applications has been shown for 3DCP combined with reinforcement and shotcreting for circular water tanks [34,35] or walls with double curvature for increased stability produced with SC3DP [14] and Mesh Mould [21]. However, despite these achievements, the potential of DFC for increasing the structural efficiency of walls is limited compared to beams and slabs, which are discussed in more detail in the following sections.

4.4. Beams

As shown in Section 3, beams offer a large potential to showcase structural efficiency. Therefore, many researchers have chosen this structural element to explore the optimisation potential of digital fabrication. In order to produce more efficient cross-sections (see Fig. 3.2), 3DCP can be applied to print hollow elements reinforced either with deformed steel reinforcement or post-tensioning. This approach was shown for beams [36,37] and short-span bridges with constant [38] and varying cross-sections [39]. The potential of KnitCrete for structurally efficient beams was demonstrated for thin-walled beams with integrated textile reinforcement [40]. The fabrication and structural performance of (double-)T-beams were explored for polymer formworks with conventional cast concrete for constant [41] as well as variable depth [42]. A parabolic depth, i.e. following the acting moment for uniform load, was also explored for a T-beam produced with 3D concrete printing and conventional reinforcement [43].

In addition to the cross-section, changing the structural system from a beam acting mainly in bending towards a system with predominant normal forces can significantly improve the structural efficiency (see Fig. 3.3 and Section 5.1). This approach was explored for 3D concrete printed trusses produced with lost formwork elements combined with conventional reinforced concrete [44], fully 3DCP trusses with external reinforcement [45–47] and reinforcement placed between the printed layers [48] (see Section 5.2). Similarly, the structural efficiency can be improved by printing filaments to follow the principal stress trajectories as shown for 3D concrete printed beams with interlayer reinforcement [49–51] and a beam cast in particle bed printed formwork [52]. Extrapolating these principles to 3D results in complex beam geometries, as demonstrated with 3DCP for a post-tensioned girder [53] and short-span bridges [54,55]. While these explorations focused on optimising the overall geometry of the beams, maintaining a rectangular outer shape and only varying the internal reinforcement layout can also increase efficiency [51], as highlighted in Section 5.3.

4.5. Slabs

Slabs offer the highest material savings potential, as they are the most mass-intense elements in common buildings [56–58]. The main potential lies in the change from a solid flat slab, where most of the applied load can be attributed to the deadweight, towards ribbed or waffle slabs - similar to the change in cross-section of beams.

Ribbed slabs are particularly efficient if the ribs enable a direct load transfer, e.g. by following the principle moment trajectories. This approach was pioneered by Pier Luigi Nervi (see Section 2) in the last century [59] and has inspired various adaptations in DFC. The geometry inspired, for example, the use of lost 3D concrete printed formworks combined with conventional reinforced concrete [60] or the fabrication

of a column slab transition with polymer formwork [41,61] (see Sections 5.4 and 5.5). Similarly, lost foam elements can be extruded and used to reduce the weight of the slab [62,63]. SC3DP was used to fabricate reinforced ribs directly on top of conventionally cast thin slab elements with different support conditions [14,64,65]. While these ribs were produced upside-down and the elements had to be turned, upstand ribs can be directly produced in their final position. Such upstand ribs were used for the Smart Slab [66]. This slab was produced with binder jetted formwork and subsequent spraying and casting. A similar concept was proposed for upstand ribs where the soffit of the slab was printed on top of a binder jetted formwork, and the ribs were fully printed [67].

Transitioning from bending active slabs towards elements mainly subjected to normal forces can be achieved with shells. Similar to a tied arch (see Fig. 3.3), shells are only activated in compression, while the tensile forces are resisted by external ties [68]. The potential of such systems produced with DFC was showcased with binder jet printed formwork [69,70] and automated concrete spraying [71,72].

5. Case studies

Each of the examples listed in the previous section has its potential and drawbacks. Elaborating on each of them is beyond the scope of this study. Therefore, in the following, the wide research area of structurally efficient elements fabricated with DFC is highlighted in five case studies covering the following areas: (i) increasing structural efficiency of reinforced concrete beams, (ii) printing structurally efficient concrete beams, (iii) improving the reinforcement layout, (iv) reaching structural efficiency at column-slab connections, and (v) applying structural efficiency through DFC to real-life projects. These case studies mainly focus on beams and slabs as these have a large savings potential.

The savings potentials indicated for the respective case studies are specific to the presented projects and chosen boundary conditions. While savings can also be achieved through other means, these shown savings highlight the potential of digital concrete to increase structural efficiency.

5.1. *Pushing the limits of optimisation for a reinforced concrete girder*

Using new materials with a reduced environmental impact, maximising the efficiency of the structures and developing novel fabrication technologies are interrelated levers towards resource-efficient concrete structures [4]. Advancements in concrete or reinforcement material technology directly lead to possible or necessary adaptations of the structural concrete element's dimensions as well as respective manufacturing processes (see Section 2). Similar interrelations apply to the use of novel digital fabrication methods such as 3D concrete printing, enabling the realisation of more complex geometries but also directly resulting in possible higher demands on used materials and challenges within application on an industrial scale, e.g. in terms of process stability. The realisation of an efficient structural concrete design raises claims to minimal tolerances in manufacturing and accurate material parameters, which may require approaches beyond conventional structural concrete design. This aspect was part of the case study presented in the following, which focuses on finding a particularly resource-efficient structural concrete girder geometry and subsequently fabricating and experimentally testing the optimised girders. Besides the presentation of the underlying methodology and the experimental results, the findings from the manufacturing process are highlighted.

The form finding of the structurally optimised concrete girder was conducted using topology optimisation tools, more precisely continuum-based approaches with minimum compliance as objective and a constraint on the volume, as well as structural layout optimisation to minimise the total volume [73]. Primarily, the material was assumed to be linear-elastic but not symmetric, meaning that a difference between tensile and compressive strength was considered. From these tools, a so-called “raw”, unprocessed design result was obtained, which was then translated into a structural concrete design. Within this step, strut-and-tie models were manually searched for to determine the flow of forces within the investigated structure, thereby facilitating the dimensioning process. In addition, design code requirements were taken into account. The development stages of the above-described form finding concept are illustrated in Fig. 5.1, starting from (top to bottom) the initial design domain (single-span girder, cross-sectional height 200 mm, depth 60 mm, span 2 m) to the raw optimisation results obtained from the mathematical optimisation tool, the extracted structural concrete design and finally a detailed view of the realised formwork and reinforcement concept.

As the case study focused on finding and experimental verification of especially resource-efficient designs rather than their optimal fabrication, the girders were conventionally cast. The materials comprised a high-performance concrete (experimentally determined cube compressive strength of approximately 90 MPa) and conventional steel reinforcement (experimentally determined yield strength of approximately 580 MPa and Young's modulus of 205 GPa).

The exploration of appropriate formwork solutions for voids sounded out several materials, such as CNC-milled timber (more details given in [74]). Satisfying results were achieved with 3D-printed PLA or CNC-milled styrofoam wrapped with smooth tape to avoid the appearance of shrinkage cracks. These void formwork elements were screwed onto the formwork's base plate (Fig. 5.1-I) of the girder, which was produced in a lying position. Another challenging aspect in the manufacturing of the structurally efficient girder was the reinforcement concept: A welded reinforcement cage was required, with internally placed reinforcing bars welded to each other and externally arranged steel plates to transfer forces within and into the structure adequately (Fig. 5.1-II). Furthermore, a fine steel mesh was wrapped around the main tensile reinforcement to serve as splitting reinforcement as well as around bars in compressive zones to ensure a more uniform crack distribution (Fig. 5.1-III). Due to the filigree dimensions of the optimised concrete girder, high geometrical accuracy was required for the reinforcement. The accuracy was substantially impaired by the limited bending radii of reinforcing bars, only gradual availability of bar diameters, and relatively high

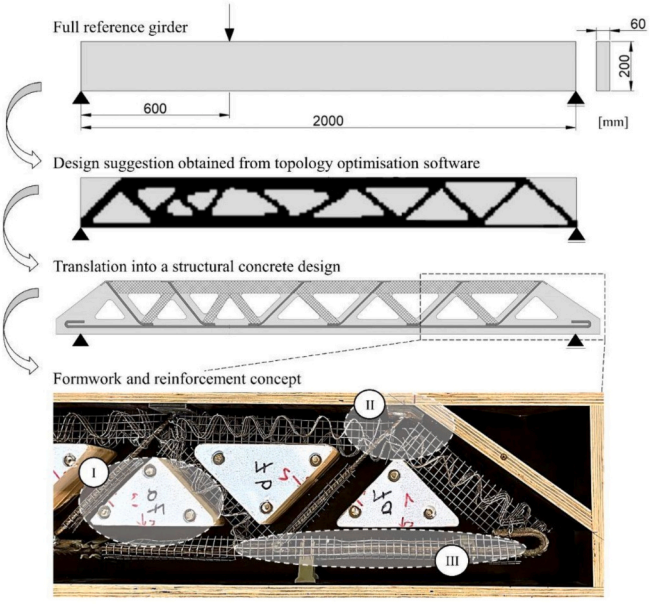

Fig. 5.1. Overview of development stages of a topology-optimised concrete girder with a detail of the formwork and reinforcement concept (I – void formwork elements produced with a CNC milling machine that are screwed onto the base formwork plate, II – conventional reinforcing bars welded to a steel plate shaped according to the outer edge of the girder, III – fine steel mesh wrapped around the main tensile reinforcement).

tolerances in the bending process and laser-cutting of steel plates. Fine-grained concrete with a maximum aggregate size of 2 mm was used to correctly fill the steel mesh with an opening width of only 10 mm.

Subsequent to a successful fabrication, the resource-efficient concrete girder was tested in a three-point bending configuration (see application of the point load in Fig. 5.1). Compared to a full, conventionally designed concrete girder, an increase in resource efficiency by almost 40 % was achieved, measured by the savings in CO_2-equivalents (Global Warming Potential of the production of concrete and reinforcement) in relation to the achieved experimental maximum load. In this context, it is particularly noteworthy that not only the load-bearing capacity but also the stiffness of the girder could be preserved or even enhanced while still guaranteeing failure announcement via sufficient yielding of the main tensile reinforcement.

The presented case study proves the realisation of a concrete girder with a significantly lower impact than a full counterpart, with more details given in [75]. This research took a conscious step away from 3D concrete printing due to challenges in reinforcement integration, process stability and the appearance of the printed results. However, the complexity of manufacturing needs to be overcome with new approaches and rethinking, e.g. in terms of conventional reinforcement strategies. Thus, the next step is to move forward from the presented artisanal case study towards an efficient, scalable digital, automated design and production process: Current research comprises [76,77] the development of an automated design tool for structurally optimised concrete girders as well as a fully robotic production process focusing on automated shuttering and casting. The design tool will implement a simplified topology optimisation applicable to the industry based on a strut-and-tie modelling approach. The manufacturing concept contains a robot fabrication cell with one or more robots working simultaneously in a precast plant or even on-site.

5.2. *Integrating 3D printing constraints into topology optimisation: Application to two-dimensional printed beams*

While the previous case study showcased the structural optimisation of beams with conventional fabrication approaches, this section addresses the possibilities of 3D concrete printing (3DCP) to produce structurally efficient beams. Topology optimisation in 3DCP can adopt various strategies, including density-based and maximum stress approaches. However, what distinguishes its application in 3DCP from conventional fabrication methods is the need to integrate technological constraints directly into the optimisation process. These constraints are central to the feasibility and success of the optimised design. They can be categorised into four broad groups, each reflecting a critical aspect of the printing process: (i) fabrication constraints, related to the capabilities of the 3D printing machinery; (ii) material constraints; (iii) construction constraints, related to the assembly and transportation of printed elements; and (iv) design constraints, related to compliance with design codes.

Several attempts have been reported to include some of these constraints in topology optimisation algorithms adopted for 3DCP. An important distinction that affects the design approach is whether they are based on (i) a three-dimensional optimisation followed by structural element segmentation or (ii) a direct print of an optimised path reflecting the most structurally efficient shape and laying in a plane. In the former case, the structure is segmented into printable cross-sections and assembled, typically by post-tensioning, to create the complete structural element [53–55]. A greater emphasis has been placed on the latter approach to accommodate printing constraints throughout the development of optimisation algorithms [78–80]. This section presents a case study consisting of the direct two-dimensional printing of a topology-optimised beam to discuss how the fabrication constraints can be implemented in the optimisation process [78].

In this case study, the non-symmetrical mechanical properties of the concrete (notably different compressive and tensile strengths) were considered in the optimisation process. Two principal fabrication constraints were integrated into the topology optimisation framework, directly associated with the characteristics of the layered extrusion process: (i) path continuity and (ii) bond of weak interfaces. The path continuity constraint (i) guarantees a continuous extrusion path for the nozzle, operated by a robotic arm, and, by extension, for the concrete filament. This factor is critical for the structural integrity of the printed object, addressing potential flaws or discontinuities in the filament's path that could compromise the structure's effectiveness. A different approach was followed within the 3DLightBeam + project [50], in which the design process included stress-driven shape optimisation to minimise the beam cross-sectional area and bending stresses and principal stress line design for determining anisotropic infill printing patterns that align with principal stress fields. Regarding weak interfaces (ii), Jewett and Carstensen [80] further explored the 3DCP constraints in terms of the mechanical effects of weak interfaces between concrete filaments, achieving designed solutions through a series of extruded filaments that form non-overlapping cores and bonding regions.

These constraints were addressed in this case study by developing a curve-based Biased Random-Key Genetic Algorithm. The topology optimisation approach was employed to optimise a simply supported solid reference beam with a rectangular cross-section of 200 × 300 mm^2 and a span of 1.8 m. The algorithm optimised stress-constrained structures to produce topologies ready for implementation without the need for post-processing. Based on this and assuming a fixed layer width of 40 mm, the algorithm provided the unreinforced solution (Fig. 5.2a) as a set of second-order Bezier curves in compliance with the path-continuity constraint. This solution allowed saving about 60 % in cementitious material volume with respect to the reference solid beam. Once the optimised shape was obtained from the algorithm, two beam specimens were printed using a 6-axis robotic arm, having a total length of 2.1 m and a maximum height of 320 mm, and made of 20 layers of 10 mm each. The two beam specimens differed by the presence or absence of steel reinforcement between layers. While the latter was used to study the type of failure of the printed element without reinforcement, the reinforced specimen yielded insight into the effect of reinforcement on the ultimate bending capacity and the potential ductile behaviour associated with the optimised shape.

Specifically, the reinforcement strategy consisted of including small-diameter steel bars into the layer plane of the optimised concrete beams, which has been observed to provide satisfactory bond strength [81]. In particular, two reinforcement layers were placed, resulting in a total geometrical reinforcement ratio of 2.5 % (referred to the concrete cross-section of 200 × 40 mm^2 of the bottom chord). This reinforcement layout derives from geometrical constraints: the reinforcing steel bars were included in the element during the printing between two consecutive layers (i.e. as a minimum distance between each other), as shown in Fig. 5.2b.

The mechanical performances of the two optimised concrete beams (unreinforced and steel reinforced) were evaluated through a three-point bending test (Fig. 5.2c). As expected, the unreinforced beam exhibited a brittle failure when the tensile strength of cementitious mortar was reached in the most loaded element (i.e. bottom chord subjected to tensile stresses). Concerning the path-optimised reinforced beam, after bottom chord tensile cracking, the interlayer reinforcement avoided failure upon crack formation, and the load could be increased until yielding was reached at a load of approximately 80 kN (i.e. almost 5 times higher than the unreinforced one). Globally, the bending tests demonstrated good flexural performance of the reinforced specimen, exhibiting a very similar load-bearing capacity (ultimate bending moment) and ductility (see crack pattern in Fig. 5.2d) as expected in conventional reinforced concrete elements. This result indicates that the optimised reinforced specimen could be designed using established conventional structural concrete design principles.

Based on this case study and recent developments in the field, it appears that the integration of topology optimisation algorithms with

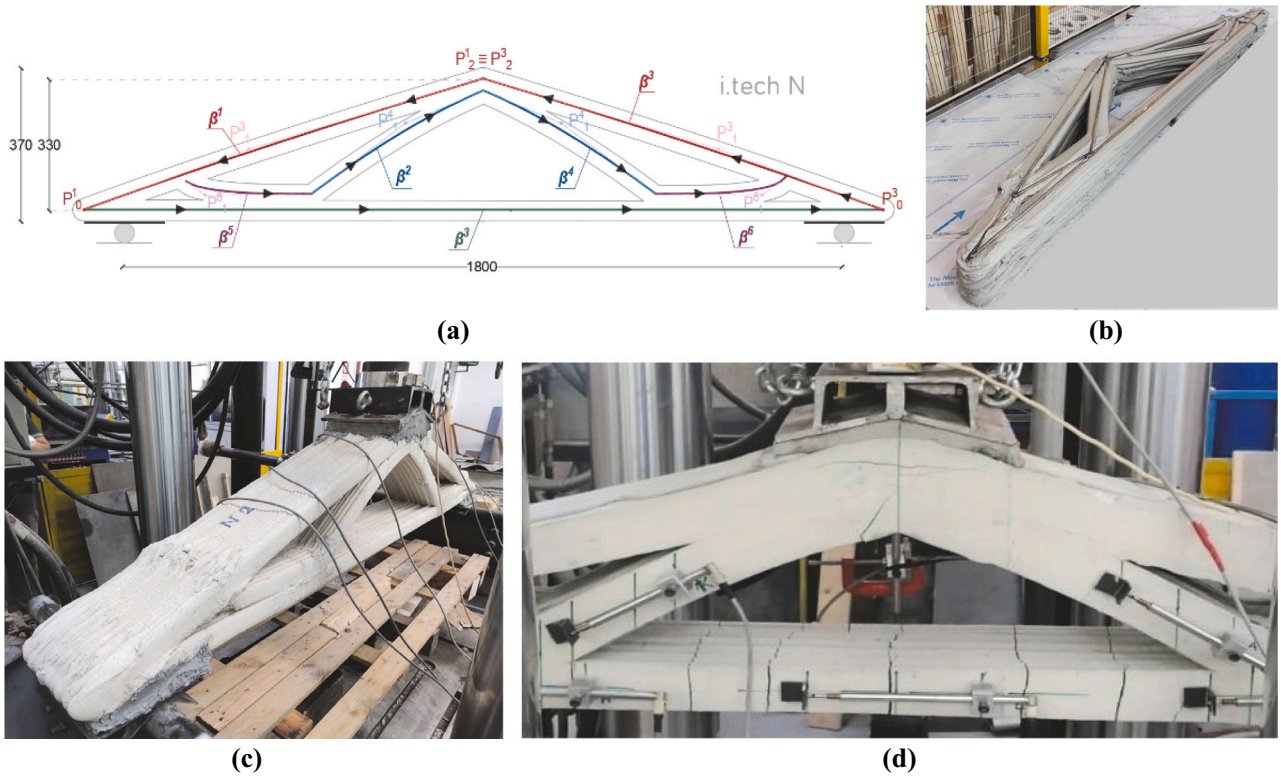

Fig. 5.2. Design, fabrication and testing of the optimised beams; (a) printing path definition through Biased Random-Key Genetic Algorithm; (b) placement of interlayer steel reinforcement; (c) test setup under three-point bending; (d) crack pattern of the steel reinforced optimised beam specimen.

the technological attributes of 3DCP has made significant advancements, increasingly minimising the need for post-processing and reaching significant reductions in material usage. However, the challenge of reinforcing optimised shapes persists, especially in matching the (complex) concrete shapes precisely. This is crucial for maintaining structural integrity and achieving the desired aesthetic and functional outcomes. As we continue to push the boundaries of 3DCP, it becomes imperative to investigate, through large-scale testing, whether these optimised designs – unlike the specimen tested in this study - introduce new modes of failure that must be considered in structural calculations. Given that optimised shapes often feature complex intersections and layer couplings, their behaviour under load may significantly differ from that of entirely solid materials (e.g. moving from flexural to shear or joint failure). Addressing these challenges is essential for advancing the capabilities of 3DCP in structural applications, ensuring that the potential for innovative design is fully realised without compromising safety or performance.

5.3. Optimising the reinforcement layout of beams

Finite element software and analyses of the stress trajectories can be used to optimise the quantities and positions of the reinforcement arrangements in reinforced concrete components. While a targeted placement of the reinforcement in the areas loaded in tension (according to common numerical analyses without constraints on reinforcement directions) in conventional formwork-based concrete construction is only possible with an enormous amount of time and additional assembly reinforcement, DFC opens up completely new opportunities for manufacturing efficiency. In 3D printing processes, the reinforcement can be automatically inserted into the concrete before, during or after the 3D printing process [64,82].

Together with digital manufacturing techniques, software-based optimisation methods enable iterative refinement of the reinforcement design based on selected variables, which is particularly beneficial for geometry-based optimisation [80]. This case study discusses a methodical procedure for optimising reinforcement layouts based on the determined principal stresses (Mohr–Coulomb theory), showing an application in beams. The beam geometry is segmented into a fine mesh, the maximum and minimum principal stresses as well as related angles are calculated, and continuous lines are formed accordingly, indicating the optimum layout of the reinforcing bars for each specimen and loading setup.

5.3.1. Beams subjected to a single static load case

In the initial step of the case study, the reinforcement of 70 × 20 × 20 cm^3 simply supported beams was optimised for a single symmetric load case, equivalent to the loading of a four-point bending test setup (Fig. 5.3a) using trajectory lines (Fig. 5.3b).

One potential solution consists of providing reinforcement following both the principal compressive stresses (red lines in Fig. 5.3b) and principal tensile stresses (blue lines in Fig. 5.3b). This approach generates a stiff steel structure inside the concrete that forms a highly efficient tied arch system (see details about the efficiency of this system in Section 3). The second reinforcement approach addresses exclusively the principal tensile stresses (blue lines in Fig. 5.3b), resulting in a reinforcement layout that complements the compressive capacity of the concrete (Fig. 5.1d) [51]. This case study used the former approach to design two optimised reinforcement layouts. A beam with a conventional reinforcement layout was also fabricated using the same concrete and reinforcement. The reinforcement amount was kept constant in all beams.

The two beams with optimised reinforcement and the reference beam with conventional reinforcement were tested until failure in a four-point bending setup (Fig. 5.3e). The beams with the optimised reinforcement layout showed a higher bending capacity compared to the reference beam thanks to the force-flow-oriented reinforcement arrangement [51]. The method presented in this case study yields the optimal reinforcing bar layout depending on the concrete properties (e.

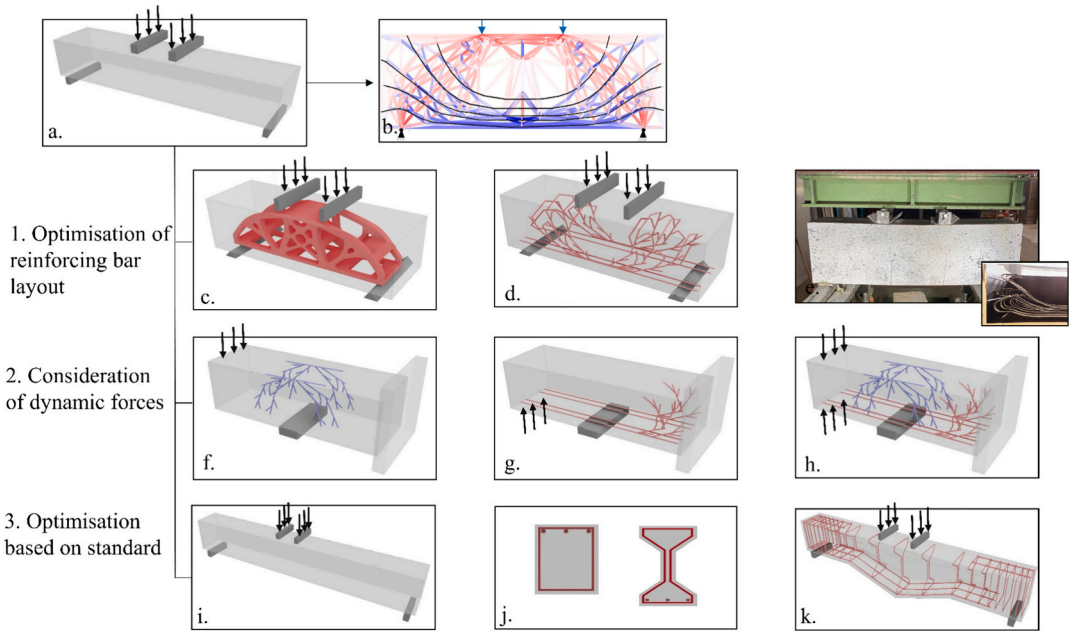

Fig. 5.3. Optimisation of a concrete beam: (a)-(d) reinforcing bar optimisation using trajectory lines for a single load; (e) fabrication and load-bearing test of the beam with optimised reinforcement; (f)-(h) consideration of loads with varying directions and positions; (i)-(k) utilisation of optimisation algorithms for concrete reduction.

g. compressive or tensile capacity) and type and magnitude of applied stresses in each zone. The approach assigns reinforcing bars to critical locations, avoids overlap, and minimises steel usage. While conventional fabrication technologies are not well suited for the resulting complex reinforcement geometries, novel digital fabrication processes can efficiently produce such optimised reinforcement layouts. However, additive manufacturing methods, like layer-by-layer concrete printing, present advantages and challenges such as attaching of shear reinforcing bars and adapting the printing process to pre-placed reinforcing bars. Various techniques have been developed to address this issue, such as adjusting the direction of the nozzle and rotating the printed element [64].

In the current case study, the printing layer of the concrete is matched with the layout of the reinforcing bars by adjusting the robot's speed and the nozzle's angle. This capability of the printing technique not only fills the spaces between the reinforcing bars but also efficiently acts as a spacer and supports layer-wise positioning of the reinforcing bars. A discussion of further developments, such as Wire Arc Additive Manufacturing of reinforcing bar layouts [83], is beyond the scope of this paper.

5.3.2. *Consideration of multiple load cases*

The previous section considered a single static load case in the optimisation. Nonetheless, the structural elements are subjected to multiple load cases in real applications. Instead of optimising based on a single load case, this demands a pragmatic approach that entails determining an envelope encompassing all load combinations and optimising based on the highest force in each element segment.

To this end, the reinforcement of a beam similar to the one analysed in Section 5.3.1 but with different boundary conditions was optimised for a time-dependent force in two directions using trajectory lines. The right side of the beam is clamped, and a one-directional pin support that exclusively carries compression is provided in the middle (Fig. 5.3f-h). At the beginning of the loading, the high shear forces near the pin support require shear reinforcing bars (Fig. 5.3f). As the direction of the load reverses and the pin support lifts off, bending becomes more prominent (Fig. 5.3g). The final reinforcement layout is obtained by combining the required reinforcement in all steps (Fig. 5.3h) [84]. The optimisation could save approximately 35 % of the reinforcements in this configuration compared to a conventional design. This highlights that the optimisation potential considering a single load case (Section 5.3.1) can only partly be exploited in real-case applications with multiple load combinations.

More details about this study can be found in [84], which details the development of codes for computing trajectory lines, facilitating the comparison of principal stress magnitudes and directions based on Mohr's Circle.

5.3.3. *Shape optimisation of the cross-section and reinforcement*

While the focus of the previous sub-chapters was exclusively on optimising the reinforcement, an optimisation to diminish the concrete volume is explored in the following. Unlike the case studies presented in Sections 5.1 and 5.2, which rely on topology optimisation tools, this research implemented metaheuristic algorithms to optimise the geometrical parameters of the cross-section and reinforcing bars simultaneously. This process consists of establishing an interface between the problem definition, which includes a design-code compliant structural analysis to estimate the load-bearing capacity, and an optimisation algorithm that selects the optimal parameters concerning the selected variables and targets. This approach was used to optimise the beam of this case study (a geometry of 110 × 20 × 20 cm^3 was used in this case; see Fig. 5.3i), where the selected parameters included the (symmetrical) cross-section geometry, stirrup distances, and the number of flexural reinforcing bars. The detailed results in [84] show that the optimisation resulted in an I-shaped cross-section at midspan that transitions to a rectangular section at the supports, which yields a 30 % reduction in concrete usage while maintaining the same load-bearing capacity (Fig. 5.3k).

5.4. *Efficient ribbed slab produced with polymer formwork*

Slabs offer the largest savings potential in building construction as they consume most materials (see Section 4.5). Therefore, this case study showcases the potential of using digitally fabricated polymer formwork in combination with conventional concrete and reinforcement to construct a part of an efficient ribbed slab inspired by the work

of Pier Luigi Nervi (see Section 2) [41,61]. The fabricated parts consisted of beams (used for preliminary tests) and a column-slab connection where the highest forces (hogging moments and punching shear) occur.

The slab was designed with a custom design-to-fabrication workflow: For a slab with constant thickness, a finite element analysis (FEA) considering linear elastic behaviour was carried out. The rib layout was then created such that the ribs aligned with the principal moment directions determined in the FEA. In an iterative process, the rib dimensions (thickness and height of ribs) and the rib spacing were optimised to minimise the material consumption while maintaining deflection limits. The reinforcement, consisting of a mesh in the solid part of the slabs, and stirrups and several layers of longitudinal reinforcement for the primary ribs, was then designed. As the polymer formwork had a thickness of only a few millimetres, special care was given to its design: With an FEA, the formwork deformations were assessed, and stiffening ribs and fixing features were designed to ensure sufficient strength and formwork stiffness. Hereby, it is notable that in contrast to previous projects applying minimal polymer formwork [11,15,31,85], which required the use of set-on-demand concrete or external counter-pressure measures, conventional self-compacting concrete without acceleration was used in this case study, causing a high formwork pressure.

Both the column-slab connections and several rib specimens with changing rib layouts (straight, kinked, curved) were fabricated as full-scale prototypes and structurally tested. All specimens were constructed upside-down in the following manner: The first 35 mm of polymer formwork were printed on an MDF print bed, whereby gaps for the reinforcement mesh were left open. The reinforcement in both orthogonal reinforcement directions was placed in these openings in two subsequent printing pauses, after which the printing of the rib walls was finished. The prefabricated rib reinforcement cages were then placed inside the rib walls, as shown in Fig. 5.4a. As the column-slab connection was designed with variable rib heights, caps were printed to close the ribs. The ribs were then cast using standard ready-mix self-compacting concrete C50/60 (maximum aggregate size $D_{max} = 8$ mm). After removal of the polymer formwork, conventional wood formwork frames were added, and the slab between the ribs was cast using low-carbon ready-mix concrete C25/30 ($D_{max} = 16$ mm). The finished specimen is shown in Fig. 5.4b. As a reference, a column-slab connection of a constant section was produced with an eccentrically placed reinforcement mesh and punching reinforcement designed according to EC2, using the same low-carbon C25/30 concrete.

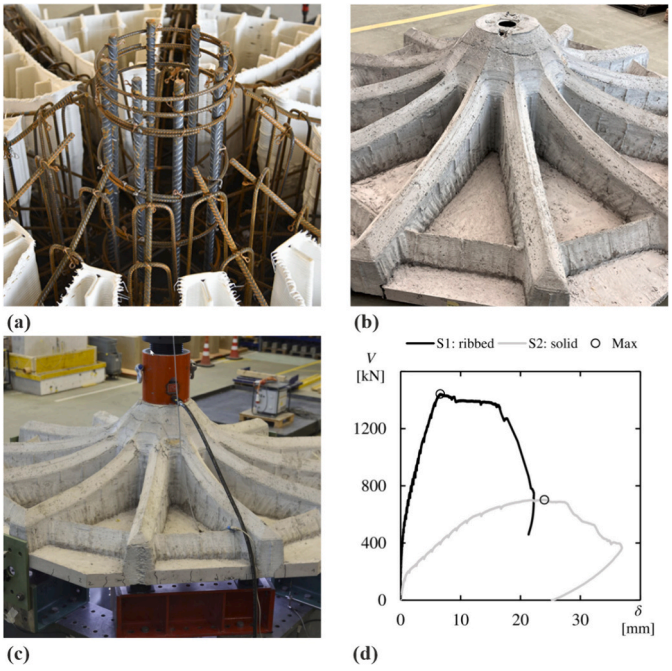

Fig. 5.4. Column-slab connection of the optimised ribbed concrete slab: (a) construction stage with finished rib walls and inserted reinforcement cages before printing of the caps [41]; (b) finished specimen [41]; (c) structural testing of specimen [61]; (d) load-deformation diagram [41].

The rib specimens were structurally tested in three-point bending, exhibiting a ductile behaviour. The specimen representing the column-slab connection of the optimised ribbed slab and the solid reference slab were structurally tested under a single, centric load with twelve equally spaced bearings (one per rib axis), as seen in Fig. 5.4c. The ribbed slab exhibited very stiff behaviour in the uncracked state and a bearing capacity almost twice as high as the solid reference slab (see Fig. 5.4d). A flexural failure mode was observed; thus, a punching failure was prevented.

As the concrete mass used for the ribbed slab was 40 % less than for the solid reference slab at similar reinforcement contents, the structural efficiency of the optimised ribbed slab was substantially superior to the solid reference slab. The significant increase in strength and stiffness despite the reduced concrete mass was due to the increase in static depth and a change in cross-section, i.e. allocating more of the concrete and reinforcement further away from the neutral axis. In this study, it was proven that digitally fabricated polymer formwork is suitable for producing design code-compliant ribbed slabs with a considerable increase in structural efficiency compared to flat slabs.

However, several difficulties were identified in the production of the specimen, the most critical being the tedious, labour-intensive removal of the formwork; several options to reduce the demoulding time and recycling of the polymer formwork are discussed in [61,86]. Further challenges must be overcome for practice applicability, such as including the connections between elements and possibly eliminating the need to rotate the specimens into the intended orientation.

5.5. *Application in practice: Bauhof Bludenz*

5.5.1. *Project overview*

A critical development for leveraging the potential of DFC to increase structural efficiency is the transition from research at a laboratory scale to real-life projects. This case study presents such a project: the “Bauhof Bludenz” recently built in Austria. The concept of this structure is to join various types of usage, such as storage and manoeuvring areas, a municipal nursery, and garages, under one roof covering approximately 700 m^2. The roof rests on two sculptural round arches spanning 46 m: a homage to the adjacent viaduct of the heritage Klarenbrunn factory's canal and, simultaneously, the structure's main static and formal element.

The initial design of the roof envisaged a monolithic slab with an average thickness of 50 cm, requiring around 360 m^3 of concrete and 53.8 t of reinforcing steel. The dead weight of the roof would have been around 70 % of the total load, meaning that most of the structural material would be required to carry its own weight. Therefore, this project provided ideal boundary conditions to explore the potential of 3DCP for large-scale structures.

With the objective to save resources and enhance the sustainability of “Bauhof Bludenz” by applying 3DCP, a collaboration between Tomaselli Gabriel Bau GmbH, Concrete 3D, gbd ZT GmbH, Baumit GmbH and the Institute for Structural Design from TU Graz was formed. With the support of TU Graz, a ceiling system was designed to save nearly 30 % of resources, using a similar system as proposed in [60]. The system consisted of customised 3D concrete printed void elements combined with conventional reinforced concrete ribs. The customisation of the void elements allowed the production of ribs following the flow of forces. Furthermore, the use of cementitious elements will enable straightforward recycling at the end of the building service life without excessive energy use.

5.5.2. Design and construction

To effectively design the slab considering the span and support conditions, the orientation of the ribs was chosen to follow the principal linear elastic moment trajectories of a monolithic slab. This process resulted in optimised and visually appealing rib orientations. Subsequently, the roof structure was pre-designed in accordance with relevant standards (such as EN1992-1-1 with Austrian national annex). This involved determining the required concrete compressive strength and reinforcement ratios.

A critical design element was the size and production of the void elements. Initially, preliminary objects were printed to determine the maximum size and weight of the elements. Subsequently, the geometry of the void elements was optimised considering various criteria, with printability, logistics and on-site handling as key factors. To ensure that the elements are printable with the available system, the stability of the elements during the print process, as well as the ideal printing speed and resulting accuracy, were determined first. Regarding logistics, the goal was to minimise the number of deliveries to the construction site without resorting to costly specialised containers but using conventional stacking pallets instead. Depending on the size of the elements, a fully loaded transport inclusive low loader was able to transport approximately 120 elements without any special permit for the transport height. Finally, the element weight was limited to 80 kg to facilitate manual handling, i.e. minimise time-intensive crane operations. Determining shape, size, weight, and arrangement of all elements accounting for these criteria was an iterative process requiring close collaboration of all stakeholders.

After the final definition of the geometry, the print paths were generated, and the void elements were prefabricated in batch operations lasting up to 52 h (see Fig. 5.5b). Printing time per void element ranged between approximately 20..45 min, depending on size. Around 35 elements were printed before rotation/storage operations could commence (approximately every 8–10 h). Subsequently, there was a brief pause for cleaning the system before resuming production. In total, 792 elements were printed with a printing path length of 210 km.

The 3D printed elements function as voids, serving both to minimise the weight of the slab and, due to their design based on force distribution, as directional elements guiding the reinforcement. The construction process was roughly as follows: After placing conventional flat slab formwork, the positions of the 3D elements were surveyed using a total station and CAD data and marked using anchor bolts. Subsequently, each element was lifted onto the formwork and placed either by crane or manually in its predefined position. One of the main challenges was the placement and alignment of the reinforcement. The reinforcement cages were fabricated on-site. Longitudinal bars for smaller radii towards the corners were chosen with a maximum diameter of Ø12 mm to facilitate on-site bending into the necessary position. The finished reinforcement cages were lifted onto the formwork and placed between the voids (see Fig. 5.5b). Based on preliminary studies, the 3D printed concrete could be accounted as concrete cover of the reinforcement. Therefore, cover spacers were only required towards the bottom of the roof. In the transverse direction, the reinforcement was then manually inserted. As the void elements were produced with the necessary slope of the top of the slab, the upper reinforcement layers could be directly placed on the voids or reinforcement cages. Finally, the ribs (space between the voids) and the top slab were cast with conventional concrete (C30/37).

With a tight timeline of 6 months from planning to execution, the project schedule was demanding. The entire project team worked tirelessly to ensure timely completion. Ultimately, the project could be finished on time, and both the client, tenants, and the project team including the construction company, 3D printing, structural engineering, and architecture, were thrilled with the design and achieved savings (see Fig. 5.5c).

5.5.3. Material efficiency

The goal of improving the material-efficiency has been successfully achieved in the construction project with a reduction of 380 tons of concrete and reinforcing steel. With a total area of 717 m^2 and

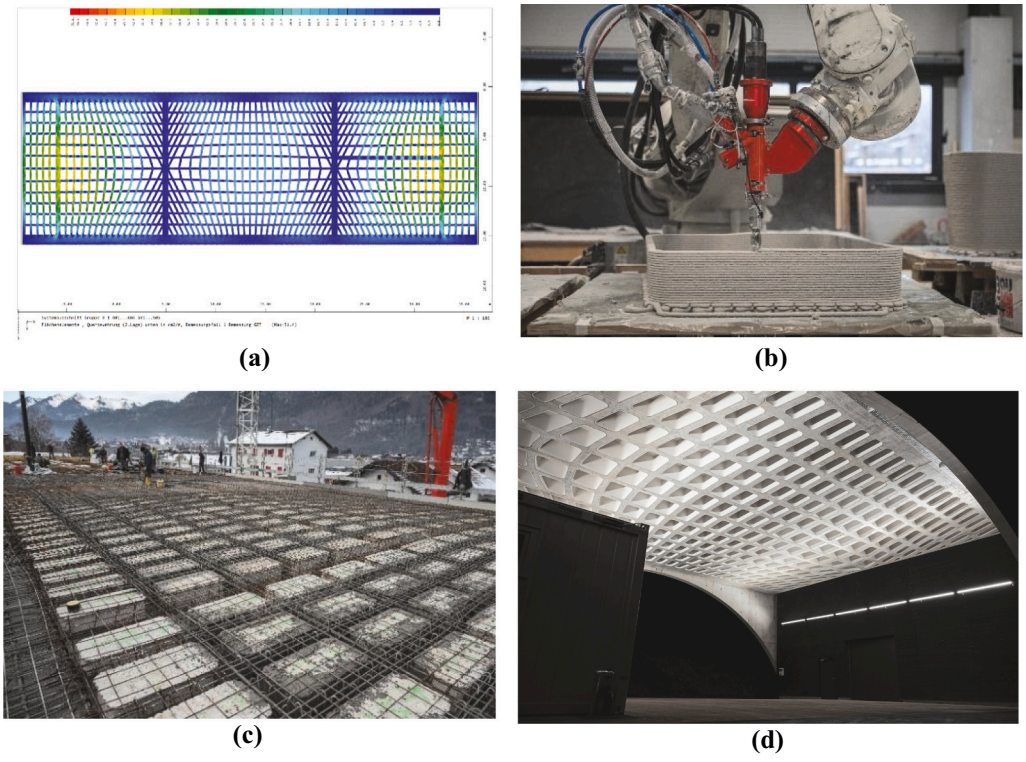

Fig. 5.5. Construction project "Bauhof Bludenz": (a) structural design; (b) printing of one void element; (c) reinforcement placement on-site; (d) finished roof (copyright: Janosch Schallert, Native Media GmbH).

dimensions measuring 46 × 14 m^2, the ceiling details exemplify this commitment to resource efficiency. Through innovative design and optimisation, significant savings compared to the reference project were realised, with a reduction by 38 % in concrete material usage, 36 % in reinforcing steel material usage (reflecting the weight savings as well as the efficient directions of ribs and thus main reinforcement), and a noteworthy decrease of 24.4 % in CO_2-equivalents despite the higher relative emissions of the 3DCP elements per mass. Notably, the utilisation of printed concrete amounted to 29.50 m^3 resulting in a void space of 155 m^3, further exemplifying the project's sustainable approach to construction.

The system has not yet been pushed to its limits, but it has demonstrated that significant material savings are possible with the help and proper application of new technologies, and that such solutions can be economically viable and result in an aesthetically convincing structure, both in terms of overall geometry as well as surface texture.

5.5.4. Outlook

The Werkhof Bludenz project aimed to demonstrate the possibilities and potentials achievable through well-conceived systems, the combination of knowledge, and new technologies that are already implementable. One critical aspect of the success of the project was the close collaboration between the general contractor (Tomaselli Gabriel Bau) and all stakeholders, as well as short communication routes. This project yielded new insights, and the system itself is continuously being developed further. Currently, there are initial attempts to minimise on-site installation effort and further utilise prefabrication. The structural system itself could also be further optimised. For instance, if the project had been executed using low-carbon concrete, there would have been even more potential for CO_2 savings. The goal of the project was not to showcase the ideal system but rather to translate research from TU Graz [60,63] into a large-scale project, with a focus on demonstrating its economic viability and competitiveness compared to other systems. This objective appears to have been met and highlights the significant potential of well-designed ceiling systems to use resources sparingly and intelligently.

6. Conclusions and outlook

Developing and implementing materials with low environmental impact, using efficient structural systems that reduce material consumption, and ensuring a long service life are crucial complementary steps towards achieving sustainable construction. While extensive research efforts to develop eco-friendly building materials have been made, optimising structural systems has not yet gathered the same attention. By ensuring a direct force flow and placing material where needed, efficient structural solutions that drastically reduce material consumption can be achieved with relative ease. The simple examples presented in this study, comparing beams with linear elastic material behaviour, highlight that in order to enhance material efficiency (i) simple solutions such as providing continuity in beams and slabs or reducing the span of the structures are very effective; (ii) where possible, the total height of the structure should be increased and efficient structural systems such as arches, trusses or deep beams should be considered; and (iii) efficient cross-sections with little material near the neutral axis (flanged or hollow cross-sections) should be used. While these principles are textbook knowledge and have been applied to countless optimised designs a century ago, they are not yet fully exploited nowadays. This unsatisfactory situation can be explained by (i) a lack of tradition of structural engineers being involved in the conceptual design phase of building structures, (ii) the underestimation of the savings potential offered by structurally efficient solutions, and (iii) the challenge of economically building material-optimised structures that often require expensive and complex formworks.

This paper addressed the second point (ii) by illustrating the tremendous savings potential of efficient structures based on simple examples that every structural engineer should be familiar with, and highlighted that digital fabrication with concrete (DFC) can tackle the third point (iii), as it comprises new technologies to produce concrete structures that are formworkless or use innovative and minimal formwork, promising to produce complex geometries minimising extra effort, cost, or waste. To this end, the opportunities and challenges of DFC in achieving sustainable construction by building with higher structural efficiency and lower material use were explored in some detail.

Several approaches to applying DFC for structurally efficient reinforced concrete elements were explored, focusing on slabs and particularly beams due to their large optimisation potential. As each approach has its advantages and drawbacks, the potential and challenges of DFC for structurally efficient reinforced concrete elements were highlighted in five case studies. These studies showed how to:

- exploit the potential to significantly increase the structural efficiency of reinforced concrete and the challenge of fabricating such complex elements,
- partly overcome these fabrication constraints by fabrication-aware optimisation with direct 3D concrete printing of truss structures with reinforcing bars between the layers,
- optimise the internal reinforcement layout,
- use polymer formworks for structurally efficient slab systems, and
- transition from laboratory scale projects to real life construction works with significant material savings.

While this small selection of case studies only shows part of a large research field, it allows identifying the potential of DFC for structurally more efficient construction. Future research should tackle the technical and organisational challenges of DFC to comply with construction mass market requirements and compare them with established efficient structural systems. In this regard, it is essential to develop processes that integrate the possibilities of robotic reinforcement assemblies and digital concrete processing. This would enable reinforcing efficiently the structural elements with the complex forms enabled by DFC and often required in material-efficient structures. While the application of 3D concrete printing to produce formworks has shown the possibilities of the technology in real-life projects, it is essential to explore new applications where digitally fabricated concrete is used structurally in order to exploit the full optimisation potential of DFC. Succeeding in these developments is required to allow digital concrete to assume a crucial role in the transition of the construction industry towards a carbon-neutral industry.

CRediT authorship contribution statement

Lukas Gebhard: Writing – review & editing, Writing – original draft, Visualization, Methodology, Investigation, Conceptualization. **Jaime Mata-Falcón:** Writing – review & editing, Writing – original draft, Visualization, Methodology, Investigation, Conceptualization. **Rebecca Ammann:** Writing – review & editing, Writing – original draft, Visualization, Software, Investigation. **Nadine Preßmair:** Writing – original draft, Investigation. **Benjamin Kromoser:** Writing – original draft, Investigation. **Costantino Menna:** Writing – review & editing, Writing – original draft, Investigation. **Abtin Baghdadi:** Writing – original draft, Investigation. **Harald Kloft:** Writing – review & editing, Writing – original draft, Investigation. **Michael Gabriel:** Writing – original draft, Investigation. **Martin Walch:** Writing – original draft, Investigation. **Walter Kaufmann:** Writing – review & editing, Writing – original draft, Investigation, Funding acquisition.

Declaration of competing interest

The authors declare that they have no known competing financial interests or personal relationships that could have appeared to influence the work reported in this paper.

Data availability

No data was used for the research described in the article.

Acknowledgements

For the project “Bauhof Bludenz” the authors want to express their gratitude to the involved parties (Client: Werit Handels GmbH, User: City of Bludenz, Architect: Atelier Ender | Architektur, General Contractor: Tomaselli Gabriel Bau, Structural Engineer: gbd ZT GmbH, Scientific Support: TU Graz, Institute for Structural Design, Manufacturing of Formworks: Concrete 3D). The research was funded by the Swiss National Science Foundation – National Centre for Competence in Research in Digital Fabrication (project number 51NF40-141853), as well as by the Deutsche Forschungsgemeinschaft (DFG, German Research Foundation) – Projektnummer 414265976 – TRR 277. Sub-project: C05-A04.

References

[1] United Nations Environment Programme, Global Status Report for Buildings and Construction, 2021, 2021.
[2] L. Gebhard, Reinforcement strategies for digital fabrication with concrete, doctoral thesis, ETH Zurich, 2023, https://doi.org/10.3929/ethz-b-000614836.
[3] R.J. Flatt, T. Wangler, On sustainability and digital fabrication with concrete, Cem. Concr. Res. (2022) 106837, https://doi.org/10.1016/j.cemconres.2022.106837.
[4] B. Kromoser, Ressourceneffizientes Bauen mit Betonfertigteilen Material – Struktur – Herstellung, in: Beton Kalender 2021, John Wiley & Sons, Ltd, 2021, pp. 305–356, https://doi.org/10.1002/9783433610206.ch3.
[5] T. Wangler, E. Lloret, L. Reiter, N. Hack, F. Gramazio, M. Kohler, M. Bernhard, B. Dillenburger, J. Buchli, N. Roussel, Digital concrete: opportunities and challenges, RILEM Tech. Lett. 1 (2016) 67–75.
[6] D. Asprone, C. Menna, F.P. Bos, T.A.M. Salet, J. Mata-Falcón, W. Kaufmann, Rethinking reinforcement for digital fabrication with concrete, Cem. Concr. Res. 112 (2018) 111–121, https://doi.org/10.1016/j.cemconres.2018.05.020.
[7] P. Marti, O. Monsch, B. Schilling, Ingenieur-Betonbau, Gesellschaft für Ingenieurbaukunst, 2005.
[8] D.P. Billington, The Art of Structural Design - a Swiss Legacy, Princeton University Art Museum, 2003.
[9] G. Gaganelis, P. Mark, P. Forman, Optimization Aided Design, Ernst & Sohn, 2022.
[10] N. Pressmair, B. Kromoser, Development stages of structurally optimised concrete girders: Design concepts, material strategies and experimental investigation, in: A. Ilki, D. Çavunt, Y.S. Çavunt (Eds.), Building for the Future: Durable, Sustainable, Resilient, Springer Nature, Switzerland, Cham, 2023, pp. 1403–1411, https://doi.org/10.1007/978-3-031-32519-9_142.
[11] E. Lloret-Fritschi, T. Wangler, L. Gebhard, J. Mata-Falcón, S. Mantellato, F. Scotto, J. Burger, A. Szabo, N. Ruffray, L. Reiter, F. Boscaro, W. Kaufmann, M. Kohler, F. Gramazio, R. Flatt, From smart dynamic casting to a growing family of digital casting systems, Cem. Concr. Res. 134 (2020) 106071, https://doi.org/10.1016/j.cemconres.2020.106071.
[12] B. Khoshnevis, Automated construction by contour crafting—related robotics and information technologies, Autom. Constr. 13 (2004) 5–19, https://doi.org/10.1016/j.autcon.2003.08.012.
[13] S. Neudecker, C. Bruns, R. Gerbers, J. Heyn, F. Dietrich, K. Dröder, A. Raatz, H. Kloft, A new robotic spray Technology for Generative Manufacturing of complex concrete structures without formwork, Procedia CIRP 43 (2016) 333–338, https://doi.org/10.1016/j.procir.2016.02.107.
[14] H. Kloft, N. Hack, J. Mainka, L. Brohmann, E. Herrmann, L. Ledderose, D. Lowke, Additive Fertigung im Bauwesen: erste 3-D-gedruckte und bewehrte Betonbauteile im Shotcrete-3-D-Printing-Verfahren (SC3DP), Bautechnik 96 (2019) 929–938, https://doi.org/10.1002/bate.201900094.
[15] A. Jipa, M. Bernhard, B. Dillenburger, Submillimeter Formwork: 3D-Printed Plastic Formwork for Concrete Elements, 2018, https://doi.org/10.3929/ETHZ-B-000237359, 13 p.
[16] J. Burger, E. Lloret-Fritschi, F. Scotto, T. Demoulin, L. Gebhard, J. Mata-Falcón, F. Gramazio, M. Kohler, R.J. Flatt, Eggshell: ultra-thin three-dimensional printed formwork for concrete structures, 3D Print. Addit. Manuf. 7 (2020) 48–59, https://doi.org/10.1089/3dp.2019.0197.
[17] D. Lowke, E. Dini, A. Perrot, D. Weger, C. Gehlen, B. Dillenburger, Particle-bed 3D printing in concrete construction – possibilities and challenges, Cem. Concr. Res. 112 (2018) 50–65, https://doi.org/10.1016/j.cemconres.2018.05.018.
[18] E. Lloret Fritschi, Smart Dynamic Casting - a Digital Fabrication Method for Non-standard Concrete Structures, Doctoral Thesis, ETH Zurich, 2016, https://doi.org/10.3929/ethz-a-010800371.
[19] M.A. Popescu, KnitCrete: Stay-in-Place Knitted Formworks for Complex Concrete Structures, ETH Zurich, 2019.
[20] N.P. Hack, Mesh Mould: A Robotically Fabricated Structural Stay-in-Place Formwork System, Doctoral Thesis, ETH Zurich, 2018.
[21] A. Mirjan, J. Mata-Falcón, C. Rieger, J. Herkrath, W. Kaufmann, F. Gramazio, M. Kohler, Mesh Mould prefabrication, in: R. Buswell, A. Blanco, S. Cavalaro, P. Kinnell (Eds.), Third RILEM International Conference on Concrete and Digital Fabrication, Springer International Publishing, Loughborough, United Kingdom, 2022, pp. 31–36, https://doi.org/10.1007/978-3-031-06116-5_5.
[22] K.E.S. Jones, M. Li, Life cycle assessment of ultra-tall wind turbine towers comparing concrete additive manufacturing to conventional manufacturing, J. Clean. Prod. 417 (2023) 137709, https://doi.org/10.1016/j.jclepro.2023.137709.
[23] K. Feickert, C.T. Mueller, Thin shell foundations: Historical review and future opportunities, in: S.A. Behnejad, G.A.R. Parke, O.A. Samavati (Eds.), Proceedings of the IASS Annual Symposium 2020/21 and the 7th International Conference on Spatial Structures, Guilford, UK, 2021, p. 14.
[24] P. Bischof, J. Mata-Falcón, J. Burger, L. Gebhard, W. Kaufmann, Experimental exploration of digitally fabricated connections for structural concrete, Eng. Struct. 285 (2023) 115994, https://doi.org/10.1016/j.engstruct.2023.115994.
[25] A. Baghdadi, M. Heristchian, H. Kloft, Connections placement optimization approach toward new prefabricated building systems, Eng. Struct. 233 (2021) 111648, https://doi.org/10.1016/j.engstruct.2020.111648.
[26] A. Baghdadi, M. Heristchian, L. Ledderose, H. Kloft, Experimental and numerical assessments of new concrete dry connections concerning potentials of the robotic subtractive manufacturing technique, Buildings 13 (2023) 210, https://doi.org/10.3390/buildings13010210.
[27] A. Baghdadi, L. Ledderose, H. Kloft, Possible geometries for precast concrete structures, through discussing new connections, robotic manufacturing and re-utilisation of the concrete elements, Buildings 14 (2024) 302, https://doi.org/10.3390/buildings14010302.
[28] E. Lloret Fritschi, F. Scotto, F. Gramazio, M. Kohler, K. Graser, T. Wangler, L. Reiter, R.J. Flatt, J. Mata Falcon, Challenges of Real-Scale Production with Smart Dynamic Casting, in: RILEM Bookseries, Springer International Publishing, 2018, pp. 299–310, https://doi.org/10.3929/ethz-b-000297640.
[29] A. Anton, P. Bedarf, A. Yoo, B. Dillenburger, L. Reiter, T. Wangler, R.J. Flatt, Concrete choreography: Prefabrication of 3D-printed columns, in: Fabricate 2020, UCL Press, 2020, pp. 286–293, https://doi.org/10.3929/ethz-b-000408884.
[30] Affentranger 3DCP, (n.d.). https://www.affentranger3dcp.ch/ (accessed July 26, 2022).
[31] J.J. Burger, E. Lloret-Fritschi, N. Taha, F. Scotto, T. Demoulin, J. Mata Falcón, F. Gramazio, M. Kohler, R.J. Flatt, Design and fabrication of a non-standard, structural concrete column using eggshell: Ultra-thin, 3D printed formwork, in: Second RILEM International Conference on Concrete and Digital Fabrication, Springer, 2020, pp. 1104–1115, https://doi.org/10.1007/978-3-030-49916-7_105.
[32] World leader in 3D construction printing, COBOD (n.d.). https://cobod.com/ (accessed March 8, 2024).
[33] Apis Cor | Construction with Robotic Precision – Apis Cor | We Print 3D Buildings, (n.d.). https://apis-cor.com/ (accessed March 8, 2024).
[34] L. Reiter, A. Anton, T. Wangler, B. Dillenburger, R.J. Flatt, A 3D printing platform for reinforced printed-sprayed concrete composites, in: R. Buswell, A. Blanco, S. Cavalaro, P. Kinnell (Eds.), Third RILEM International Conference on Concrete and Digital Fabrication, Springer International Publishing, Cham, 2022, pp. 249–254, https://doi.org/10.1007/978-3-031-06116-5_37.
[35] L. Gebhard, J. Mata-Falcón, A. Iqbal, W. Kaufmann, Structural behaviour of post-installed reinforcement for 3D concrete printed shells – a case study on water tanks, Construct. Build Mater. 366 (2023) 130163, https://doi.org/10.1016/j.conbuildmat.2022.130163.
[36] L. Gebhard, J. Mata-Falcón, A. Anton, B. Dillenburger, W. Kaufmann, Structural behaviour of 3D printed concrete beams with various reinforcement strategies, Eng. Struct. 240 (2021) 112380, https://doi.org/10.1016/j.engstruct.2021.112380.
[37] R. Yu, A Digital Workflow for the Design and Manufacturing of 3D Printed Concrete Bridges in a Circular Economy: Structural Design Considerations for Pre-Stressed Beams and Dry Connections, Technische Universiteit Eindhoven, 2022.
[38] T.A.M. Salet, Z.Y. Ahmed, F.P. Bos, H.L.M. Laagland, Design of a 3D printed concrete bridge by testing, Virtual Phys. Prototyp. 13 (2018) 222–236, https://doi.org/10.1080/17452759.2018.1476064.
[39] Z. Ahmed, R. Wolfs, F. Bos, T. Salet, A Framework for Large-Scale Structural Applications of 3D Printed Concrete: the Case of a 29 m Bridge in the Netherlands, in: Open Conference Proceedings, 2022, pp. 5–19, https://doi.org/10.52825/ocp.v1i.74.
[40] M. Lee, J. Mata-Falcón, M. Popescu, W. Kaufmann, Thin-walled concrete beams with stay-in-place flexible formworks and integrated textile shear reinforcement, Struct. Concr. 24 (2023) 4960–4977, https://doi.org/10.1002/suco.202200648.
[41] T. Huber, J. Burger, J. Mata-Falcón, W. Kaufmann, Structural design and testing of material optimized ribbed RC slabs with 3D printed formwork, Struct. Concr. 24 (2023) 1932–1955, https://doi.org/10.1002/suco.202200633.
[42] L. Gebhard, J. Burger, J. Mata-Falcón, E. Lloret Fritschi, F. Gramazio, M. Kohler, W. Kaufmann, Towards efficient concrete structures with ultra-thin 3D printed formwork: exploring reinforcement strategies and optimisation, Virtual Phys. Prototyp. 17 (2022) 599–616, https://doi.org/10.1080/17452759.2022.2041873.
[43] L. Gebhard, P. Bischof, A. Anton, J. Mata-Falcón, B. Dillenburger, W. Kaufmann, Pre-installed reinforcement for 3D concrete printing, in: R. Buswell, A. Blanco, S. Cavalaro, P. Kinnell (Eds.), Third RILEM International Conference on Concrete and Digital Fabrication, Springer International Publishing, Loughborough, United Kingdom, 2022, pp. 430–435, https://doi.org/10.1007/978-3-031-06116-5_64.
[44] S. Maitenaz, R. Mesnil, A. Feraille, J.-F. Caron, Materialising structural optimisation of reinforced concrete beams through digital fabrication, Structures 59 (2024) 105644, https://doi.org/10.1016/j.istruc.2023.105644.

[45] N. Pressmair, B. Kromoser, Pushing concrete material usage to the limit: weight optimised, 3D printed concrete girders with external reinforcement, 2021, p. 528, https://doi.org/10.35789/fib.PROC.0055.2021.CDSymp.P064.
[46] D. Asprone, C. Menna, F. Bos, J. Mata-Falcón, L. Ferrara, F. Auricchio, E. Cadoni, V. M.C.F. Cunha, L. Esposito, A. Fromm, S. Grünewald, H. Kloft, V. Mechtcherine, V. N. Nerella, R. Schipper, Structural design and testing of digitally manufactured concrete structures, in: N. Roussel, D. Lowke (Eds.), Digital Fabrication with Cement-Based Materials, Springer International Publishing, Cham, 2022, pp. 187–222, https://doi.org/10.1007/978-3-030-90535-4_6.
[47] minimass — minimum construction for maximum development, (n.d.). https://www.minimass.net/ (accessed September 2, 2022).
[48] C. Menna, L. Esposito, Flexural behaviour of steel-reinforced topology-optimised beams fabricated by 3D concrete printing, in: R. Buswell, A. Blanco, S. Cavalaro, P. Kinnell (Eds.), Third RILEM International Conference on Concrete and Digital Fabrication, Springer International Publishing, Cham, 2022, pp. 404–410, https://doi.org/10.1007/978-3-031-06116-5_60.
[49] L. Breseghello, R. Naboni, Toolpath-based design for 3D concrete printing of carbon-efficient architectural structures, Addit. Manuf. 56 (2022) 102872, https://doi.org/10.1016/j.addma.2022.102872.
[50] L. Breseghello, H. Hajikarimian, H.B. Jørgensen, R. Naboni, 3DLightBeam+. Design, simulation, and testing of carbon-efficient reinforced 3D concrete printed beams, Eng. Struct. 292 (2023) 116511, https://doi.org/10.1016/j.engstruct.2023.116511.
[51] R. Dörrie, N. Freund, E. Herrmann, A. Baghdadi, I. Mai, F. Galli, M. David, K. Dröder, D. Lowke, H. Kloft, Automated force-flow-oriented reinforcement integration for shotcrete 3D printing, Autom. Constr. 155 (2023) 105075, https://doi.org/10.1016/j.autcon.2023.105075.
[52] D. Kovaleva, M. Nistler, A. Verl, L. Blandini, W. Sobek, Zero-waste production of lightweight concrete structures with water-soluble sand formwork, in: R. Buswell, A. Blanco, S. Cavalaro, P. Kinnell (Eds.), Third RILEM International Conference on Concrete and Digital Fabrication, Springer International Publishing, Cham, 2022, pp. 3–8, https://doi.org/10.1007/978-3-031-06116-5_1.
[53] G. Vantyghem, W. De Corte, E. Shakour, O. Amir, 3D printing of a post-tensioned concrete girder designed by topology optimization, Autom. Constr. 112 (2020) 103084, https://doi.org/10.1016/j.autcon.2020.103084.
[54] K. Kinomura, S. Murata, Y. Yamamoto, H. Obi, A. Hata, Application of 3D printed segments designed by topology optimization analysis to a practical scale Prestressed pedestrian bridge, in: F.P. Bos, S.S. Lucas, R.J.M. Wolfs, T.A.M. Salet (Eds.), Second RILEM International Conference on Concrete and Digital Fabrication, Springer International Publishing, Cham, 2020, pp. 658–668, https://doi.org/10.1007/978-3-030-49916-7_66.
[55] T. Ooms, G. Vantyghem, Y. Tao, M. Bekaert, G. De Schutter, K. Van Tittelboom, W. De Corte, The production of a topology-optimized 3D-printed concrete bridge, in: R. Buswell, A. Blanco, S. Cavalaro, P. Kinnell (Eds.), Third RILEM International Conference on Concrete and Digital Fabrication, Springer International Publishing, Cham, 2022, pp. 37–42, https://doi.org/10.1007/978-3-031-06116-5_6.
[56] B. Regúlez, D.M.V. Faria, L. Todisco, M. Fernández Ruiz, H. Corres, Sustainability in construction: the urgent need for a new ethics, Struct. Concr. 24 (2023) 1893–1913, https://doi.org/10.1002/suco.202200406.
[57] J. Mata-Falcón, P. Bischof, T. Huber, A. Anton, J. Burger, F. Ranaudo, A. Jipa, L. Gebhard, L. Reiter, E. Lloret-Fritschi, T. Van Mele, P. Block, F. Gramazio, M. Kohler, B. Dillenburger, T. Wangler, W. Kaufmann, Digitally fabricated ribbed concrete floor slabs: a sustainable solution for construction, RILEM Tech. Lett. 7 (2022) 68–78, https://doi.org/10.21809/rilemtechlett.2022.161.
[58] P. Bischof, J. Mata-Falcón, W. Kaufmann, Fostering innovative and sustainable mass-market construction using digital fabrication with concrete, Cem. Concr. Res. 161 (2022) 106948, https://doi.org/10.1016/j.cemconres.2022.106948.
[59] P.L. Nervi, Costruire correttamente, Hoepli, Milano, 1955.
[60] G. Hansemann, R. Schmid, C. Holzinger, J. Tapley, K. Hoang Huy, V. Sliskovic, B. Freytag, A. Trummer, S. Peters, Additive fabrication of concrete elements by robots - lightweight concrete ceiling, in: J. Burry, J. Sabin, B. Sheil, M. Skavara (Eds.), Fabricate 2020, UCL Press, 2020.
[61] J. Burger, T. Huber, E. Lloret-Fritschi, J. Mata-Falcón, F. Gramazio, M. Kohler, Design and fabrication of optimised ribbed concrete floor slabs using large scale 3D printed formwork, Autom. Constr. 144 (2022) 104599, https://doi.org/10.1016/j.autcon.2022.104599.
[62] P. Bedarf, Robotic 3D Printing of Mineral Foam for a Lightweight Composite Concrete Slab, in: Jeroen van Ameijde, Nicole Gardner, Kyung Hoon Hyun, Dan Luo, Urvi Sheth (Eds.), POST-CARBON - Proceedings of the 27th CAADRIA Conference, Sydney, 9–15 April 2022, CUMINCAD, 2022, pp. 61–70, https://doi.org/10.52842/conf.caadria.2022.2.061.
[63] R. Schmid, G. Hansemann, M. Autischer, J. Juhart, Adaptive foam concrete in digital fabrication, in: R. Buswell, A. Blanco, S. Cavalaro, P. Kinnell (Eds.), Third RILEM International Conference on Concrete and Digital Fabrication, Springer International Publishing, Cham, 2022, pp. 22–28, https://doi.org/10.1007/978-3-031-06116-5_4.
[64] H. Kloft, M. Empelmann, N. Hack, E. Herrmann, D. Lowke, Reinforcement strategies for 3D-concrete-printing, Civ. Eng. Des. 2 (2020) 131–139, https://doi.org/10.1002/cend.202000022.
[65] Y. Xiao, N. Hack, H. Kloft, Digital structural design and shotcrete 3D printing strategies for lightweight reinforced concrete beam-grid structures, in: Proceedings for the 6th Fib International Congress, Oslo, Norway, 2022.
[66] M.A. Meibodi, A. Jipa, R. Giesecke, D. Shammas, M. Bernhard, M. Leschok, K. Graser, B. Dillenburger, Smart Slab. Computational design and digital fabrication of a lightweight concrete slab, in: ACADIA//2018: Recalibration. On Imprecisionand Infidelity. [Proceedings of the 38th Annual Conference of the Association for Computer Aided Design in Architecture (ACADIA) ISBN 978–0–692-17729-7] Mexico City, Mexico 18–20 October, 2018, CUMINCAD, 2018, pp. 434–443, https://doi.org/10.52842/conf.acadia.2018.434.
[67] A. Anton, A. Jipa, L. Reiter, B. Dillenburger, Fast complexity: Additive manufacturing for prefabricated concrete slabs, in: F.P. Bos, S.S. Lucas, R.J. M. Wolfs, T.A.M. Salet (Eds.), Second RILEM International Conference on Concrete and Digital Fabrication, Springer International Publishing, Cham, 2020, pp. 1067–1077, https://doi.org/10.1007/978-3-030-49916-7_102.
[68] A. Liew, D.L. López, T. Van Mele, P. Block, Design, fabrication and testing of a prototype, thin-vaulted, unreinforced concrete floor, Eng. Struct. 137 (2017) 323–335, https://doi.org/10.1016/j.engstruct.2017.01.075.
[69] A. Jipa, C. Calvo Barentin, G. Lydon, M. Rippmann, G. Chousou, M. Lomaglio, A. Schlueter, P. Block, B. Dillenburger, 3D-Printed Formwork for Integrated Funicular Concrete Slabs, 2019.
[70] F. Ranaudo, T. Van Mele, P. Block, A Low-Carbon, Funicular Concrete Floor System: Design and Engineering of the HiLo Floors, in: Ghent, Belgium, 2021, pp. 2016–2024, https://doi.org/10.2749/ghent.2021.2016.
[71] M. Nuh, R. Oval, J. Orr, P. Shepherd, Digital fabrication of ribbed concrete shells using automated robotic concrete spraying, Addit. Manuf. (2022) 103159, https://doi.org/10.1016/j.addma.2022.103159.
[72] R. Oval, M. Nuh, E. Costa, O.A. Madyan, J. Orr, P. Shepherd, A prototype low-carbon segmented concrete shell building floor system, Structures 49 (2023) 124–138, https://doi.org/10.1016/j.istruc.2023.01.063.
[73] N. Stoiber, B. Kromoser, Topology optimization in concrete construction: a systematic review on numerical and experimental investigations, Struct. Multidiscip. Optim. 64 (2021) 1725–1749, https://doi.org/10.1007/s00158-021-03019-6.
[74] N. Stoiber, B. Kromoser, Putting structurally optimised concrete girders to the test: Design, Manufacture & Experimental Investigation, in: Proceedings Fib Congress 2022 Oslo - Concrete Innovation for Sustainability, Oslo, 2022, p. 10.
[75] N. Pressmair, Investigations on Topology-Optimised, Resource-Efficient Concrete Girders, University of Natural Resources and Life Sciences, 2023.
[76] P. Gappmaier, S. Reichenbach, B. Kromoser, Automated production process for structure-optimised concrete elements, in: A. Ilki, D. Çavunt, Y.S. Çavunt (Eds.), Building for the Future: Durable, Sustainable, Resilient, Springer Nature, Switzerland, Cham, 2023, pp. 1577–1585, https://doi.org/10.1007/978-3-031-32511-3_161.
[77] B. Kromoser, P. Gappmaier, I. Ahmed, S. Reichenbach, Automated design and production of structurally optimised reusable concrete building elements: Introduction of a concept to decrease the environmental impact and increase the economic potential in concrete construction, (Under review).
[78] T. Pastore, C. Menna, D. Asprone, Bézier-based biased random-key genetic algorithm to address printability constraints in the topology optimization of concrete structures, Struct. Multidiscip. Optim. 65 (2022) 64, https://doi.org/10.1007/s00158-021-03119-3.
[79] M. Bi, P. Tran, L. Xia, G. Ma, Y.M. Xie, Topology optimization for 3D concrete printing with various manufacturing constraints, Addit. Manuf. 57 (2022) 102982, https://doi.org/10.1016/j.addma.2022.102982.
[80] J.L. Jewett, J.V. Carstensen, Topology-optimized design, construction and experimental evaluation of concrete beams, Autom. Constr. 102 (2019) 59–67, https://doi.org/10.1016/j.autcon.2019.02.001.
[81] L. Gebhard, C. Laura Esposito, J. Mata-Falcón Menna, Inter-laboratory study on the influence of 3D concrete printing set-ups on the bond behaviour of various reinforcements, Cem. Concr. Compos. 133 (2022) 104660, https://doi.org/10.1016/j.cemconcomp.2022.104660.
[82] V. Mechtcherine, R. Buswell, H. Kloft, F.P. Bos, N. Hack, R. Wolfs, J. Saranjan, B. Nematollahi, E. Ivaniuk, T. Neef, Integrating reinforcement in digital fabrication with concrete: a review and classification framework, Cem. Concr. Compos. (2021) 103964, https://doi.org/10.1016/j.cemconcomp.2021.103964.
[83] A. Baghdadi, C. Müller, H. Kloft, Potentials of 3D printing technique in optimum Design of Reinforced-Concrete Elements, in: IASS Annual Symposia 2019, 2019.
[84] A. Baghdadi, R. Dörrie, H. Kloft, New calculation approach for selecting and orienting the reinforcing material for robotic concrete manufacturing, 2020, pp. 1–11.
[85] L. Reiter, T. Wangler, A. Anton, R.J. Flatt, Setting on demand for digital concrete – principles, measurements, chemistry, validation, Cem. Concr. Res. 132 (2020) 106047, https://doi.org/10.1016/j.cemconres.2020.106047.
[86] J. Burger, E. Lloret-Fritschi, M. Akermann, D. Schwendemann, F. Gramazio, M. Kohler, Circular formwork: recycling of 3D printed thermoplastic formwork for concrete, Technology|Architecture + Design 7 (2023) 204–215, https://doi.org/10.1080/24751448.2023.2245724.